

# Effect of TiO<sub>2</sub> nanoparticle doping on the performance of electrically-controlled nematic liquid crystal core waveguide switch



Mukesh Sharma, Aloka Sinha\*, M.R. Shenoy

Department of Physics, Indian Institute of Technology Delhi, Hauz Khas, New Delhi 110 016, India

## ARTICLE INFO

### Article history:

Received 12 June 2015

Received in revised form 31 August 2015

Accepted 10 September 2015

Available online 1 October 2015

### Keywords:

Liquid crystal devices

Dielectric anisotropy

Titanium dioxide nanoparticles

Electro-optical waveguide devices

Optical switching devices

## ABSTRACT

A liquid crystal (LC) core waveguide has been designed and fabricated using nanocolloid of the nematic liquid crystal 5CB, doped with TiO<sub>2</sub> nanoparticles, as the core. Nematic liquid crystals doped with small amount of nanoparticles can have significantly altered electro-optic response. The performance of the fabricated LC core waveguide as an optical-switch has been studied, and the experimental result shows that the threshold voltage for switching is reduced from 1 V to 0.25 V due to TiO<sub>2</sub> nanoparticle dopant-concentration of 2.0 wt.%. The overall optimal performance of the waveguide switch, in terms of threshold voltage, extinction ratio, and response time, is achieved for a dopant-concentration of 0.5 wt.%.

© 2015 Elsevier B.V. All rights reserved.

## 1. Introduction

Optical waveguides are the building blocks of any integrated optical device; these also provide optical connection between different functional devices, forming an integrated optical circuit. The advantages of an integrated optical circuit are compact size, planar geometry with multiple waveguides on one chip, higher efficiency, lower power consumption, and provision for integration of the devices [1]. Liquid crystal (LC) waveguides find applications in integrated optical devices, primarily as optical switch, due to their high birefringence and electro-optical characteristics [2,3]. Various geometries of nematic LC core waveguides on different substrates, such as silicon [4,5] and glass [6,7] have been proposed. Low operating voltage with negligible power dissipation is a strong requirement for LC core waveguide based devices. In recent years, the affect of doping of LC with nanoparticles has been extensively studied [8]. Doping with nanoparticles can change the performance characteristics of LCs, such as electro-optic and dielectric properties, memory effect, and phase behavior. Various types of nanoparticles such as metallic [9], semiconducting [10], ferroelectric [11,12], carbon nano-tubes [13,14], dielectric and insulating [15–19] have been developed in recent years to realize LC nanocolloids. Several reports [20–22] have shown that doping of a nematic LC with small

amounts of nanoparticles affects the properties of nematic LC such as the decrease of threshold and switching voltages, and switching time of the device. The insulating nanoparticles of titanium dioxide (TiO<sub>2</sub>) have attracted much attention for many device applications due to their physical, chemical and electrical properties [23]. Lee et al. [24] reported the enhancement of electro-optic performance of a LC system by the addition of TiO<sub>2</sub> nanoparticles in the nematic LC. They demonstrated that the threshold voltage of the LC for device operation is reduced from 2.5 V to 0.5 V due to the addition of TiO<sub>2</sub> nanoparticles up to 2.0 wt.%. Chen et al. [19] reported that doping by TiO<sub>2</sub> nanoparticles reduce the impurity-ion concentration in a LC cell which is responsible for the lower threshold voltage of the device. The decrease in the threshold voltage of LC can result in a reduction in the power consumption. Thus, the study of the LC core waveguides, designed using nanocolloids is interesting for the realization of future power saving LC core waveguide devices.

In this paper, we report fabrication and characterization of LC core waveguides in which the core region is filled with nanocolloids of the liquid crystal 5CB, doped with TiO<sub>2</sub> nanoparticles. Three nanocolloids with concentrations of 0.5 wt.%, 1.0 wt.% and 2.0 wt.% TiO<sub>2</sub> nanoparticles in 5CB are prepared. The effect of the variation of the dopant concentration on the electro-optic characteristics and threshold voltage for switching of the LC core waveguide has been presented. In Section 2 we describe the fabrication of LC core waveguide and preparation of nanocolloids of different concentrations. Results and discussion are presented in Section 3.

\* Corresponding author.

E-mail address: [alokaphysics@gmail.com](mailto:alokaphysics@gmail.com) (A. Sinha).

2. Experiment

2.1. Fabrication of LC core waveguide switch and the experimental setup

The LC core waveguide comprises of two ITO-coated glass plates, which form the upper and lower cladding layers, and are separated by a 5 μm thick layer of negative photoresist (AZ15nXT), which determines the thickness of the waveguide (see Fig. 1). The nematic LC 5CB is used as the waveguide core material, with ordinary ( $n_o$ ) and extraordinary ( $n_e$ ) refractive indices of 1.53 and 1.71, respectively, at 632.8 nm [2]. The fabricated waveguide structure is a rectangular core waveguide with a guiding layer of thickness 5 μm, width = 2 mm and length = 5 mm. The ITO layer (on the glass plate) is a conducting film which is used as the electrodes of the LC core waveguide. For homogeneous alignment of the LC molecules, a polyimide layer was spin-coated at 4000 rpm over both ITO-coated glass substrates, and was ‘rubbed’ along the length of the waveguide using velvet cloth.

A schematic of the experimental setup is shown in Fig. 2. In the experiment, a He-Ne laser at the wavelength of 632.8 nm is used as the light source. The plane of polarization of the input light is controlled by a half-wave plate (HWP), and a 20× microscope objective (MO) is used to couple light into the LC core waveguide. To study the transmission characteristics of the LC core waveguide switch, a square wave voltage signal of frequency 1 kHz is applied across the electrodes of the device. The output of the waveguide was collected by a 20× MO, and it is measured by a power meter attached to a photodetector.

2.2. Preparation of TiO<sub>2</sub>: 5CB nanocolloids

Initially, three nanocolloids of LC doped with TiO<sub>2</sub> nanoparticle were prepared, with concentrations of 0.5 wt.%, 1.0 wt.%, and 2.0 wt.%, respectively. TiO<sub>2</sub> nanoparticles, which were obtained from Sigma Aldrich, USA, have a particle size of the order of ~21 nm. To prepare each nanocolloid, a fixed amount of TiO<sub>2</sub> nanoparticles were first mixed in the 5CB LC, and then chloroform was added to the LC + TiO<sub>2</sub> mixture. The mixture was ultrasonicated for 10 min to allow the TiO<sub>2</sub> nanoparticles to disperse

uniformly into the 5CB, and then the solution was kept on a hot plate at 60 °C for 6 h. This process was repeated two times to obtain a uniform nanocolloid. Finally, the chloroform was evaporated from the pure LC + TiO<sub>2</sub> mixture at this temperature. The above process was followed to prepare 0.5 wt.%, 1.0 wt.%, and 2.0 wt.% concentrations of LC nanocolloids. The core region was filled as required with pure 5CB and the three prepared samples of LC + TiO<sub>2</sub> nanocolloids by capillary action [7].

3. Results and discussion

3.1. Electro-optic and dielectric anisotropy studies

In the experiment, the switching characteristics of the doped LC core waveguide are studied for TE (horizontal) and TM (vertical) polarizations of input light [7]. The measured output power variations for pure 5CB and the prepared nanocolloids of different dopant concentration (0.5 wt.%, 1.0 wt.% and 2.0 wt.%) with applied voltage are shown in Fig. 3.

As can be seen from Fig. 3, the output power drops when the applied voltage exceeds the threshold voltage for the TM polarization, and there is very little change in the output power for the TE polarization. The V-parameter defines the total number of modes supported by the waveguide [1], and the numerical value of V-parameter is larger for the TM mode, since  $n_e > n_o$ . With the applied electric field, the coupled power in the TM polarization is distributed among the various modes due to the increased V-parameter of the waveguide. The output power drops at the threshold voltage for the TM polarization due to the higher absorption coefficient of the TM modes in the metal-clad waveguide [7].

When an external electric field is applied to the LC layer, the LC molecules reorient because of their dielectric anisotropies; dielectric interaction between the LC molecules and the applied electric field. A rotation of the LC molecules generates a translational motion of the molecules, which produces a torque, which in turn affects the rotation of the molecules. Under a given electric field, the liquid crystal will be in the equilibrium state where the total free energy is minimized. If the dielectric anisotropy is positive ( $\Delta\epsilon > 0$ ), the LC molecules tend to align parallel to the applied electric field. The LC molecules tend to align perpendicular to the applied electric field when the dielectric anisotropy is negative ( $\Delta\epsilon < 0$ ). This field-induced reorientation of the LC molecules is referred to as the Freedericksz transition. The threshold voltage (Freedericksz transition voltage) for the LC is given by [2]

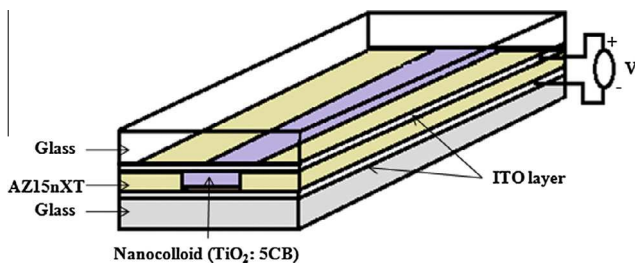


Fig. 1. Schematic of the LC core waveguide, filled with nanocolloid (TiO<sub>2</sub>: 5CB) in the core region.

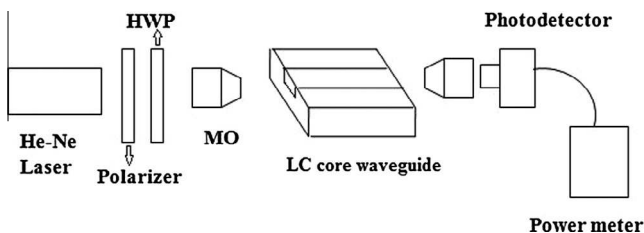


Fig. 2. Schematic diagram of the experimental setup to characterize the LC core waveguide. HWP: Half-wave plate; MO: Microscope objective (20×).

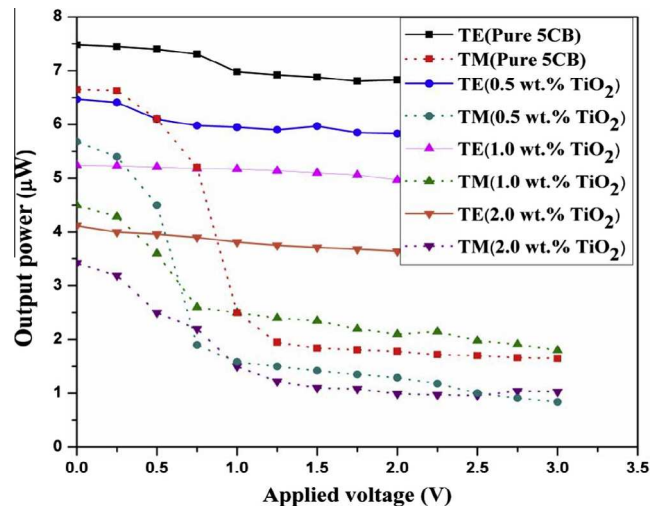


Fig. 3. Variation of output power with applied voltage for pure LC, and the nanocolloids 0.5 wt.%, 1.0 wt.% and 2.0 wt.% TiO<sub>2</sub> doping concentrations in 5CB.

$$V_{th} = \pi \sqrt{K_{11} / \epsilon_0 \Delta \epsilon} \quad (1)$$

where ' $K_{11}$ ' is the elastic constant for deformation, ' $\Delta \epsilon$ ' is the dimensionless dielectric anisotropy parameter and ' $\epsilon_0$ ' is the free-space dielectric permittivity. From Eq. (1), one can see that the threshold voltage for re-orientation of LC molecules depends on the dielectric anisotropy. The dielectric anisotropy ' $\Delta \epsilon = \epsilon_{||} - \epsilon_{\perp}$ ' of the nematic LC indicates to the anisotropic nature of the molecules, where ' $\epsilon_{||}$ ' and ' $\epsilon_{\perp}$ ' are the components parallel and perpendicular to the molecular long axis, respectively [2]. The dielectric anisotropy is an important parameter that defines the lower threshold voltage for LC devices. After the addition of  $\text{TiO}_2$  nanoparticles, there is a strong dipolar interaction between the  $\text{TiO}_2$  molecules and the nematic LC which can induce the desired dielectric anisotropy and relaxation parameters of the LC. In order to obtain the numerical value of dielectric anisotropy of the LC, the capacitance of the liquid crystal cell is measured as a function of applied voltage, using a LCR meter (Agilent E4980A), and the dielectric constant ( $\epsilon$ ) is plotted as a function of voltage for two different frequencies (see Fig. 4).

From Fig. 4, at applied voltages lower than the threshold voltage, the measured dielectric constant is ' $\epsilon_{\perp}$ ' and at applied voltages much higher than the threshold voltage, the measured dielectric constants are ' $\epsilon_{||}$ ' [25]. The dielectric anisotropy ' $\Delta \epsilon = \epsilon_{||} - \epsilon_{\perp}$ ' were then obtained. The value of  $\Delta \epsilon$  of LC doped with  $\text{TiO}_2$  nanoparticles is higher than the pure 5CB LC (see Fig. 4). Thus, from Eq. (1), it can be seen that there is a reduction of the threshold voltage in doped LC, in comparison to pure LC. For 0.5 wt.%, 1.0 wt.%, and 2 wt.%  $\text{TiO}_2$

nanocolloids, the measured threshold voltages were  $0.70 V_{pp}$ ,  $0.55 V_{pp}$ , and  $0.25 V_{pp}$ , respectively, which are lower compared to the threshold voltage of  $1 V_{pp}$  for the pure 5CB LC core waveguide, as can be seen in Fig. 3. Thus, the reduction in the threshold voltage for the waveguide switch is because of  $\text{TiO}_2$  nanoparticle dopants, which changes the dielectric anisotropy. The dielectric anisotropy of the  $\text{TiO}_2$  doped 5CB LC is higher compared to pure 5CB LC. This behavior shows the dependence of the dielectric constant ( $\epsilon$ ) on the concentration of  $\text{TiO}_2$  molecules which is shown in Fig. 4. The dielectric constant is measured at the frequency of 1 kHz (frequency of applied voltage), and also at a higher frequency of 1 MHz. From Fig. 4, we can see that both pure and doped LC exhibit positive dielectric anisotropy. The dielectric anisotropy is increased in the case of doped LC, while beyond a few volts, no significant change in the dielectric constant is observed with the applied voltage at both frequencies.

The experimental results for the threshold voltage and extinction ratio (i.e. the ratio of the two power levels of TE and TM polarizations [7]) of the LC core waveguide are shown in Table 1.

The size and concentration of the  $\text{TiO}_2$  nanoparticles in the nanocolloids play a critical role in the electro-optic response of this material [21]. The light propagation characteristics of both pure and doped samples are qualitatively similar (see Fig. 3). This also implies that  $\text{TiO}_2$  nanoparticles are well-mixed with the 5CB molecules, and a combined molecular re-orientation occurs. In the case of ITO coated glass substrates with 'rubbing' on inner sides, the pretilt angle (i.e. average upward tilt angle of the molecules with reference to the alignment layer) of the nanocolloids is increased. With the increase in the  $\text{TiO}_2$  doping concentration, two effects occur: First, the threshold voltage for switching decreases with the increase in doping concentration because of the increase in the number of insulating  $\text{TiO}_2$  nanoparticles. These nanoparticles trap more number of the moving ion impurities that flow toward the alignment layers [19,21]. Second, the output power drops slowly over a wider range of applied voltage, for higher concentrations of nanoparticles. The high concentration doping of the nanoparticles in LC (i.e. for 2.0 wt.%), disturbs the orientational ordering of the molecules which results in the disturbance of both the director and order parameter of LC. The change in the order parameter of LC, results in an increase in the total free energy of the system. For compensation of these energy expenses, aggregation of nanocolloids is triggered. The nanocolloids begin to approach each other and form aggregates. The rate of formation of aggregates is directly proportional to the doping concentration of nanoparticles [26]. Thus, there is an increase in the rotational viscosity of the nanocolloid comprising of spherical shaped  $\text{TiO}_2$  nanoparticles [27]. Although the threshold voltage is reduced, the complete molecular re-orientation of the nanocolloid occurs at a relatively higher applied voltage, which can be seen from Fig. 3.

The reduction of threshold voltage is also due to reduced screening effect, which is caused by the flowing ions in the LC layer [24]. Before applying the voltage across the waveguide switch, the ion impurities adsorbed on the alignment layer creates an inner direct current field and decreases the effective voltage of the nematic LC layer [19]. This screening effect increases the threshold voltage required for the LC based device. The doping of insulating nanocolloids provides traps for ions in the LC layer; therefore fewer ions flow to the alignment layer, which leads to reduction in the screening effect, and a corresponding reduction in the threshold voltage of the device.

Therefore, a combination of the above effects results in the decrease in the threshold voltage of LC core waveguide. The measured threshold voltage for 0.5 wt.%  $\text{TiO}_2$  nanocolloid doped LC core waveguide is  $0.7 V_{pp}$ , which is less compared to  $1.0 V_{pp}$  for pure 5CB LC core waveguide as shown in Fig. 5. As the doping concentration of nanocolloids increases, the aggregation of

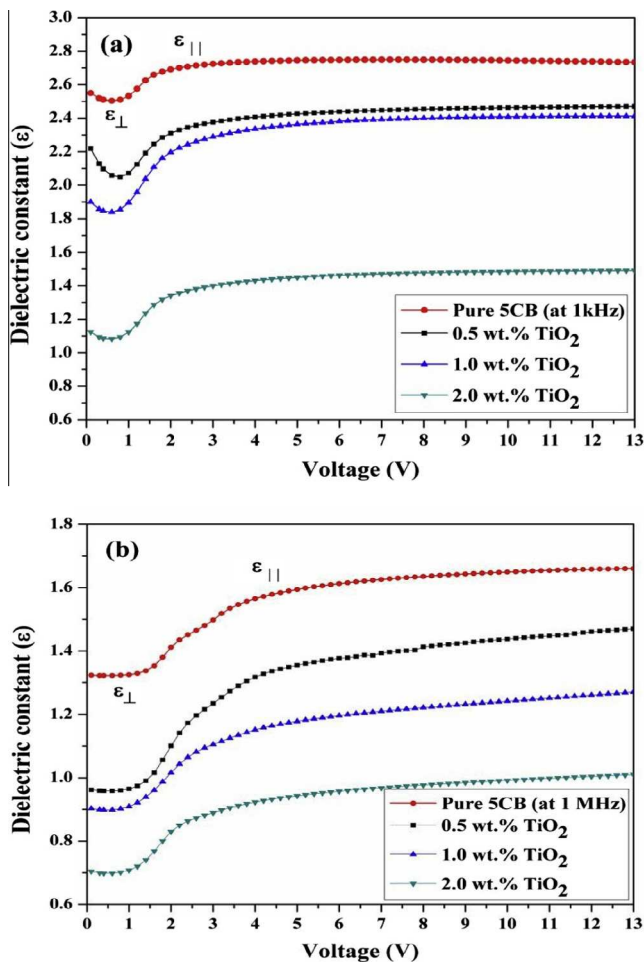


Fig. 4. Variation of dielectric constant with voltage (a) at frequency of 1 kHz, and (b) at frequency of 1 MHz, for different  $\text{TiO}_2$  doping concentrations.

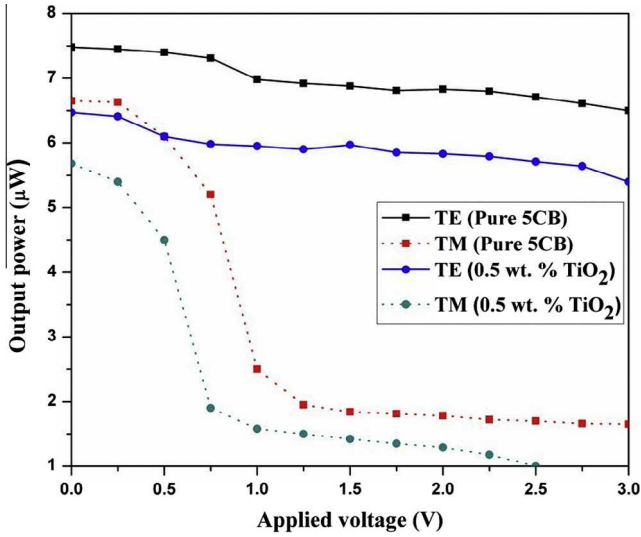


Fig. 5. Variation of output power with applied voltage for 0.5 wt.% TiO<sub>2</sub> doped LC core waveguide.

nanocolloids also increases [26]. As can be seen from Fig. 3, the output power does not drop sharply (i.e. reduce over a wider range of voltage) in case of higher nanocolloid concentration of 2.0 wt.% TiO<sub>2</sub>; this is because in the case of higher concentration of nanoparticles, the rate of formation of aggregates is higher. But in the case of 0.5 wt.% TiO<sub>2</sub>, the output power drops sharply at a threshold voltage (see Fig. 3) which indicates that there is less effect of the aggregation of the nanocolloid. Due to the above combined effects, the measured extinction ratio and the differential attenuation are highest for 0.5 wt.% TiO<sub>2</sub> nanocolloid, among the different nanocolloids considered (1.0 wt.% TiO<sub>2</sub>, 2.0 wt.% TiO<sub>2</sub>), which is shown in Table 1. Thus, 0.5 wt.% TiO<sub>2</sub> doped 5CB shows the optimum performance in terms of threshold voltage and switching characteristics.

3.2. Response time

Fig. 6 shows the snapshots of the display screen of the digital storage oscilloscope (DSO) showing the response of the LC core waveguide to an applied square wave voltage. The rise and fall times have been calculated as the time taken for the output voltage to change from 10% to 90% and 90% to 10% of its maximum value, respectively. As shown in Fig. 6, for 0.5 wt.%, 1.0 wt.%, and 2.0 wt.% TiO<sub>2</sub> doping, the measured rise times were 10.8 ms, 15.6 ms, and 19.4 ms, respectively. The corresponding fall times were 31.2 ms,

Table 1

Variation of threshold voltage, extinction ratio and differential attenuation for the LC core waveguide as a function of TiO<sub>2</sub> doping concentration.

S. No.	Sample + doping concentration	Threshold voltage V <sub>th</sub> (V <sub>pp</sub> )	Extinction ratio	Differential attenuation for TM polarization
1.	Pure 5CB	1.0	7.1 dB	5.2 dB
2.	5CB + 0.5 wt.% TiO <sub>2</sub>	0.70	6.6 dB	4.8 dB
3.	5CB + 1.0 wt.% TiO <sub>2</sub>	0.55	4.6 dB	4.1 dB
4.	5CB + 2.0 wt.% TiO <sub>2</sub>	0.25	4.2 dB	3.8 dB

10 ms, and 8 ms, respectively. The rise time for doped samples increases with TiO<sub>2</sub> doping concentration. Compared to pure LC core waveguide, both rise and fall times are higher for the doped LC core waveguide. As discussed above, the change in rise and fall times for the doped LC core waveguide is due to the change in rotational viscosity of the doped LC molecules.

3.3. Estimation of the attenuation coefficients

In metal clad (ITO layer, in this case) waveguides, the attenuation of TM modes is greater than TE modes, and the attenuation coefficients of the higher order modes are larger as compared to that of lower order modes [28]. Due to the change in dielectric anisotropy of the 5CB LC after doping, the refractive indices of 5CB also changes; we measured the change in refractive index by using an Abbe refractometer at the wavelength of 633 nm. The ordinary refractive indices for doped LC were found to be 1.56, 1.581 and 1.602 for 0.5 wt.%, 1.0 wt.%, and 2.0 wt.% TiO<sub>2</sub> doped LC, respectively. Due to increased refractive indices, the total number of modes supported by the waveguide is increased. The attenuation coefficient for the TE and TM modes are approximately given by [29]:

$$\alpha_{TEm} \approx \frac{(m + 1)^2 \pi^2}{n_f k^2 d^3} \left[ \frac{\epsilon_i}{(n_f^2 - \epsilon_r)^{3/2}} \right] \tag{2}$$

$$\alpha_{TMm} \approx \frac{(m + 1)^2 \pi^2}{n_f k^2 d^3} \left[ \frac{\epsilon_i (2n_f^2 - \epsilon_r)}{n_f^2 (n_f^2 - \epsilon_r)^{3/2}} \right] \tag{3}$$

where ‘m’ is the mode number, ‘n<sub>f</sub>’ is the refractive index of the nanocolloids, ‘ε<sub>r</sub>’ and ‘ε<sub>i</sub>’ are the real and imaginary parts of the dielectric constant of the metal (for metals, |ε<sub>r</sub>| ≫ ε<sub>i</sub>), and ‘d’ is the thickness of the LC film. Using the numerical values ε<sub>r</sub> = −3.46 and ε<sub>i</sub> = 0.22 (for the ITO layer) at 633 nm [30], the calculated attenuation coefficient for TE and TM modes are given by:

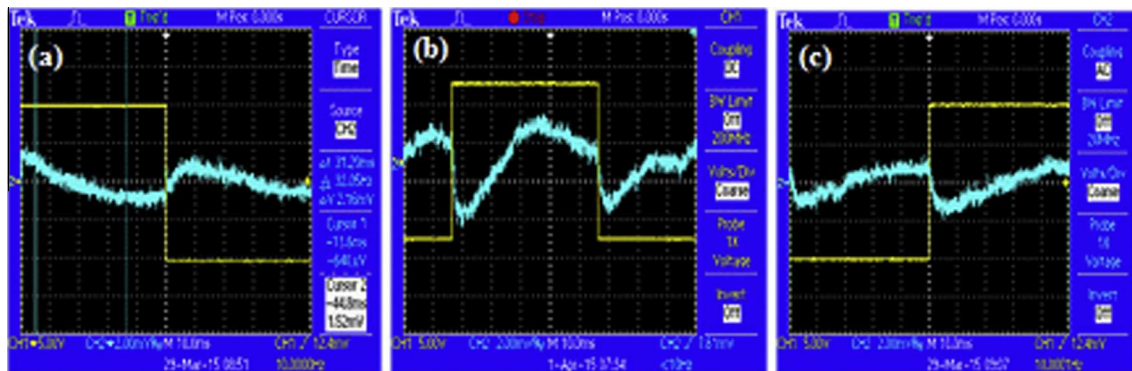


Fig. 6. Snapshots of the display screen of the DSO showing the response of the LC core waveguide to an applied square wave voltage: (a) 0.5 wt.% TiO<sub>2</sub>, (b) 1.0 wt.% TiO<sub>2</sub>, (c) 2.0 wt.% TiO<sub>2</sub> doped LC core waveguides.

$\alpha_{TEm} = 0.076(m + 1)^2 \text{ (cm}^{-1}\text{)}$ ,  $\alpha_{TMm} = 0.258(m + 1)^2 \text{ (cm}^{-1}\text{)}$ . In this case, the attenuation coefficient of TM modes is 3.38 times greater than that for the TE modes. The above estimated attenuation coefficient for the TE and TM modes are consistent with measured differential output which can be seen in Table 1 and Fig. 3.

#### 4. Conclusion

We have studied switching characteristics of the LC core waveguides, realized using nanocolloids of the nematic LC 5CB. The electro-optic characteristics of TiO<sub>2</sub> doped 5CB LC core waveguides have been experimentally investigated. As the TiO<sub>2</sub> doping concentration is increased, the dielectric anisotropy increases, and the screening effect of the alignment layer is reduced; this leads to a lower threshold voltage for the LC core waveguide switch. Study of the propagation characteristics of TE and TM polarizations in the doped LC core waveguides with different doping concentration, indicate that the optimal performance, in terms of lower threshold and differential attenuation, is obtained for 0.5 wt.% TiO<sub>2</sub> doped LC core waveguide. The nanoparticle doped LC core waveguides are potential candidates for differential loss-switching devices with very low threshold voltage.

#### References

- [1] A.K. Ghatak, K. Thyagarajan, *Optical Electronics*, Cambridge Univ. Press, Cambridge, U.K., 1989.
- [2] I.C. Khoo, *Liquid Crystals*, second ed., Wiley, New York, NY, USA, 2007.
- [3] A. Miniewicz, A. Gniewek, J. Parka, *Opt. Mater.* 21 (2002) 605–610.
- [4] A. d'Alessandro, B. Bellini, D. Donisi, R. Beccherelli, R. Asquini, *IEEE J. Quantum Electron.* 42 (2006) 1084–1090.
- [5] D. Donisi, B. Bellini, R. Beccherelli, R. Asquini, G. Gilardi, M. Trotta, A. d'Alessandro, *IEEE J. Quantum Electron.* 46 (2010) 762–768.
- [6] T.J. Wang, C.K. Chung, W.J. Li, T.J. Chen, B.Y. Chen, *J. Lightw. Technol.* 31 (2013) 3570–3574.
- [7] M.R. Shenoy, M. Sharma, A. Sinha, *J. Lightw. Technol.* 33 (2015) 1948–1953.
- [8] See, e.g., the Review Paper by F.-H. Lin, C.-Y. Ho, J.-Y. Lee, *Opt. Mater.* 34 (2012) 1181–1194.
- [9] Y. Shiraiishi, N. Toshima, K. Maeda, H. Yoshikawa, J. Xu, S. Kobayashi, *Appl. Phys. Lett.* 81 (2002) 2845.
- [10] T. Zhang, C. Zhong, J. Xu, *Jpn. J. Appl. Phys.* 48 (2009) 055002.
- [11] J.-F. Blach, S. Saitzek, C. Legrand, L. Dupont, J.-F. Henninot, M. Warengem, *J. Appl. Phys.* 107 (2010) 074102.
- [12] A. Lorenz, N. Zimmermann, S. Kumar, D.R. Evans, G. Cook, H.-S. Kitzerow, *Phys. Rev. E* 86 (2012) 051704.
- [13] R. Basu, G.S. Iannacchione, *Phys. Rev. E* 81 (2010) 051705.
- [14] L. Petti, M. Rippa, A. Fiore, L. Manna, P. Mormile, *Opt. Mater.* 32 (2010) 1060–1065.
- [15] P. Malik, K.K. Raina, *Opt. Mater.* 27 (2004) 613–617.
- [16] P.-S. Chen, C.-C. Huang, Y.-W. Liu, C.-Y. Chao, *Mol. Cryst. Liq. Cryst.* 507 (2009) 202–208.
- [17] N. Topnani, V. Hamplova, M. Kaspar, V. Novotna, E. Gorecka, *Liq. Cryst.* 41 (2014) 91–100.
- [18] G. Nabil, W.F. Ho, H.P. Chan, *Appl. Opt.* 52 (2013) E15–E21.
- [19] W.-T. Chen, P.-S. Chen, C.-Y. Chao, *Mol. Cryst. Liq. Cryst.* 507 (2009) 253–263.
- [20] C.-Y. Tang, S.-M. Huang, W. Lee, *J. Phys. D: Appl. Phys.* 44 (2011) 355102.
- [21] T.-R. Chou, J. Hsieh, W.-T. Chen, C.-Y. Chao, *Jpn. J. Appl. Phys.* 53 (2014) 071701.
- [22] S.K. Gupta, D.P. Singh, R. Manohar, *Adv. Mater. Lett.* 6 (2015) 68–72.
- [23] Y.-S. Ha, H.-J. Kim, H.-G. Park, D.-S. Seo, *Opt. Exp.* 20 (2012) 6448.
- [24] W.-K. Lee, J.-H. Choi, H.-J. Na, J.-H. Lim, J.-M. Han, J.-Y. Hwang, D.-S. Seo, *Opt. Lett.* 34 (2009) 3653–3655.
- [25] F. Yakuphanoglu, M. Okutan, O. Koysal, S.-M. Ahn, S.R. Keum, *Dyes Pigments* 76 (2008) 721–725.
- [26] Q. Li, *Liquid Crystal Beyond Displays: Chemistry, Physics, and Applications*, John Wiley & Sons, New Jersey, 2012.
- [27] N. Podoliak, O. Buchnev, M. Herrington, E. Mavrona, M. Kaczmarek, A.G. Kanaras, E. Stratakis, J.-F. Blach, J.-F. Henninot, M. Warengem, *RSC Adv.* 4 (2014) 46068.
- [28] Z. Shi, Q. Guo, *J. Lightw. Technol.* 27 (2009) 3135–3141.
- [29] C.L. Chen, *Propagation loss in thin-film waveguides*, Foundations for Guided-Wave Optics, Wiley, New York, NY, USA, 2007, pp. 77–92.
- [30] J.A. Dobrowolski, *Handbook of Optics*, second ed., McGraw Hill, USA, 1995.